RSC Advances

ROYAL SOCIETY OF CHEMISTRY

www.rsc.org/advances

ARTICLE TYPE www. rsc.org/xxxxxx | XXXXXXXX

Dual-frequency Microwave-driven Resonant Excitations of Skyrmions in Nanoscale magnet

Han Wang, Yingying Dai, Teng Yang, Weijun Ren and Zhidong Zhang*

Received Xth XXXXXXXXXX 20XX, Accepted Xth XXXXXXXXX 20XX
First published on the web Xth XXXXXXXXXX 200X
DOI:10.1039/b000000x

Since the first prediction of its existence in magnetic materials, skyrmion has been intensively investigated from theoretically to experimentally. However, it remains a challenge to manipulate skyrmion and to understand its dynamics. We study nonlinear dynamics of coupled skyrmions in Co/Ru/Co nanodisks by micromagnetic simulation and show that resonant excitations can be controlled in nanoscale by a dual-frequency microwave field. Two coupled resonant modes, clockwise (CW) and counter-clockwise (CCW) rotation modes, are found. Polygon-like resonant excitations are observed and modulated from triangle-like to heptagon-like dynamics by a microwave field with commensurate frequency ratio. Quasiperiodic behavior of excitations are related to an incommensurate ratio. We also present numerical solutions of the extended Thiele's equation for skyrmion and obtain a good agreement between the solutions and the micromagnetic simulation results. This work contributes to the understanding of skyrmion dynamics and supplies a new route to manipulating skyrmion in nanoscale using resonant excitations.

1 Introduction

Nanoscale magnets have aroused much attention in recent years due to their unique magnetic properties sensitive to the geometrical parameters of magnets.[1–4] For example, scaling a magnet down from bulk to nanofilm will lead to a strong shape anisotropy. As the geometric size scales down further, many peculiar properties will emerge, such as a single-domain state from a multidomain one, topological spin textures and so on.[1,5–7] Topological spin textures among them are especially intriguing due to its potential applications in high-density data storage, microwave devices and spintronics, because of their nanoscale size, non-volatility and high speed operation.[8–10]

Skyrmion as one type of the topological spin textures has recently been observed experimentally in chiral-lattice magnets,[11–17] and also predicted to exist in coupled ordinary magnets.[18–20] Skyrmion is envisioned promising candidate for applications in spintronics and magnetic storage,[8,21,22] due to its small size, high structural stability, low threshold current density to drive its motion, and intriguing magnetoelectric effect.[12,22–24] Therefore, besides spin-polarized current,[25–27] searching other methods of efficiently manipulating skyrmion in nanoscale and understanding the dynamics of skyrmion, particularly at resonant excitations, are important subjects for practical applications.

Many research works on the resonant excitations of vortex with a topological spin texture have been carried out in recent years, showing that the vortex core can be switched even with low power consumption and nanostructural magnets with topological spin textures have potential applications in microwave sources and resonators.[9,10,28–30] However, resonant excitations of skyrmion have seldom been reported. In our recent work, skyrmion under resonant excitations has shown dual-frequency flower-like dynamics when driven by a single-frequency microwave field, which is ascribed to its nonlocal deformation of topological density distribution.[31] It is therefore curious and worthwhile to investigate skyrmion motion in a dual-frequency microwave driving field, which is of great importance to a further understanding of the behaviors under the resonant excitations and may supply a more facile way to manipulating skyrmion for applications.

In this work, we present an approach for manipulating topological resonant excitations of coupled skyrmions in nanoscale by a dual-frequency microwave field. We find two resonant modes with opposite direction of rotation in a single-frequency microwave field. The two modes have dynamically coupled phase under a dual-frequency field, which has not been discovered before. By modulating the commensurate ratio of the dual-frequencies, we obtain polygon-like resonant excitation and are able to controllably change it. Quasiperiodic behavior is observed when the frequency ratio is incommensurate. Numerical solutions to the extended Thiele's equation are in best agreement with the micromagnetic simulation results and verifies that the effective mass is vital to the polygon-like resonant excitations of skyrmion as well as the value of frequency and the frequency ratio of the external field. We

Shenyang National Laboratory for Materials Science, Institute of Metal Research and International Centre for Materials Physics, Chinese Academy of Sciences, 72 Wenhua Road, Shenyang 110016, PRC. Fax: +86-24-23891320; Tel: +86-24-23971859; E-mail: zdzhang@imr.ac.cn

also show the perpendicular coupling between two skyrmions has a great effect on skyrmion dynamics.

2 Methods

Resonant excitation of coupled skyrmions in Co/Ru/Co nanodisks was studied by means of the three-dimensional object oriented micromagnetic framework (OOMMF) code.[32] The material parameters of hexagonal-close-packed (hcp) cobalt chosen include the saturation magnetization M_s=1.4×10^6 A/m, the exchange stiffness A_{ex}=3×10^{-11} J/m and the uniaxial anisotropy constant K_u=5.2×10^5 J/m^3 with the direction perpendicular to the nanodisk plane. The interfacial coupling constant of the adjacent surfaces was -5×10^{-5} J/m^2 according to ref. 33. A dimensionless damping α was 0.02. The radius R of a Co/Ru/Co nanodisk was 100 nm. The thickness L of Co was 18 nm, while that of Ru was 2 nm. The cell size was 2×2×2 nm^3, which is smaller than the exchange length of cobalt (about 4.94 nm). The method of obtaining static coupled skyrmions was the same as our previous work:[18] Different initial magnetic states (vortex-like, in-plane-like, and out-of-plane-like initial states) were used to obtain the most stable state. The in-plane microwave field was applied to static coupled skyrmions in x-direction to active the resonant excitations of the coupled skyrmions. The frequency of the external field is equal or close to the eigenfrequency of the system. The waveforms of microwave fields are $Hsin(2\pi ft)$ with frequency of 1 GHz or 5 GHz and $H_1 sin(2\pi f_1 t) + H_2 sin(2\pi f_2 t)$ with f_1/f_2 of 1/2, 1/3, 1/4, 1/5, 1/6 or golden ratio, respectively.

3 Results and Discussion

3.1 Effective mass

Deformation of a skyrmion at resonance will be large nonlocal because of its smooth global spin texture. To consider the nonlocal nature of large deformation, we use guiding center (the center of topological density) to depict its dynamics[34]. The local magnetization $\boldsymbol{S}(\boldsymbol{x},t)$ depends not only on guiding center's position $\boldsymbol{R}(t)$ but also on its velocity $\dot{\boldsymbol{R}}(t)$,[35] we can get:

$$\boldsymbol{S}(\boldsymbol{x},t) = \boldsymbol{S}(\boldsymbol{x} - \boldsymbol{R}(t), \dot{\boldsymbol{R}}(t)), \tag{1}$$

Then we are able to obtain the extended Thiele's equation of the guiding center:

$$-\partial U/\partial \boldsymbol{R} + \mu \boldsymbol{H} + \boldsymbol{G} \times \dot{\boldsymbol{R}} = \hat{\boldsymbol{e}}_i M_{ij} \ddot{R}_j, \tag{2}$$

where $\boldsymbol{G}$ is the gyrovector, $\hat{\boldsymbol{e}}_i$ unit coordinate vector $(i(j) = x, y)$, coefficient μ a function of structural and magnetic parameters,[36,37], $\boldsymbol{H}$ an external magnetic field and M the effective mass tensor with elements:

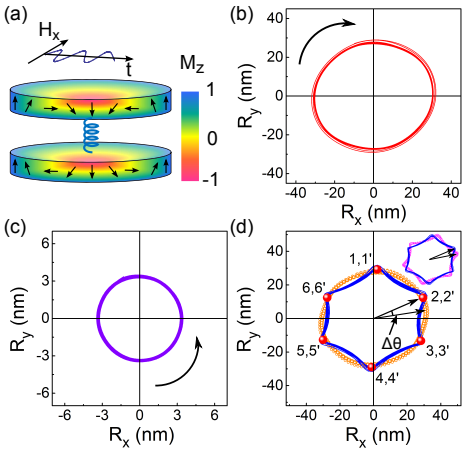

Fig. 1 (Color online) (a) The sketch of two coupled skyrmions with opposite chiralities in a Co/Ru/Co nanodisk. (b), (c) and (d) are the trajectories of the skyrmion on the top nanolayer in a single-frequency field of 1 GHz (b), 5 GHz (c), and a dual-frequency field with the ratio f_1/f_2 of 1/5 and H_1/H_2 of 5/1 (d), respectively. The orange dot line and the pink dot line in the inset are the sum of orbits of 1 GHz and 5 GHz with amplitude ratio of 5/1 and 1/1, respectively. Curved arrows represent the sense of rotation. Numbers in (d) label the cusps of the hexagon during two periods. Amplitude of H_1 is 100 Oe.

$$M_{ij} = -\gamma^{-1} S \int d^2x \boldsymbol{n} \cdot (\frac{\partial \boldsymbol{n}}{\partial x_i} \times \frac{\partial \boldsymbol{n}}{\partial \dot{R}_j}), \tag{3}$$

where γ the gyromagnetic ratio and $\boldsymbol{n}$ the unit vector of local magnetization. The potential energy of the guiding centers is:

$$U = \frac{1}{2} k \boldsymbol{R}_t^2 + \frac{1}{2} k \boldsymbol{R}_b^2 + U_{Sky-Sky}(d), \tag{4}$$

where k, $d = |\boldsymbol{R}_t - \boldsymbol{R}_b|$, and $U_{Sky-Sky}(d)$ are stiffness coefficient, the distance of two guiding centers, and the magnetostatic coupling between two skyrmions, respectively. For a skyrmion with a nonlocal deformation of topological object, the effective mass, which is related to the time derivative of topological density $\dot{q}$,[35] has to be used to comprehend the dynamical behaviors of the skyrmion.

3.2 Results of Micromagnetic simulations

Resonant excitations of the two coupled skyrmions are stimulated by a microwave magnetic field as shown in Fig. 1. The field is 100 Oe of amplitude and applied along the +x direction on the top nanolayer as shown in Fig. 1a. Trajectories of the guiding center for the top nanolayer in the field $Hsin(2\pi ft)$ with frequencies of 1 GHz and 5 GHz are shown in Figs. 1b

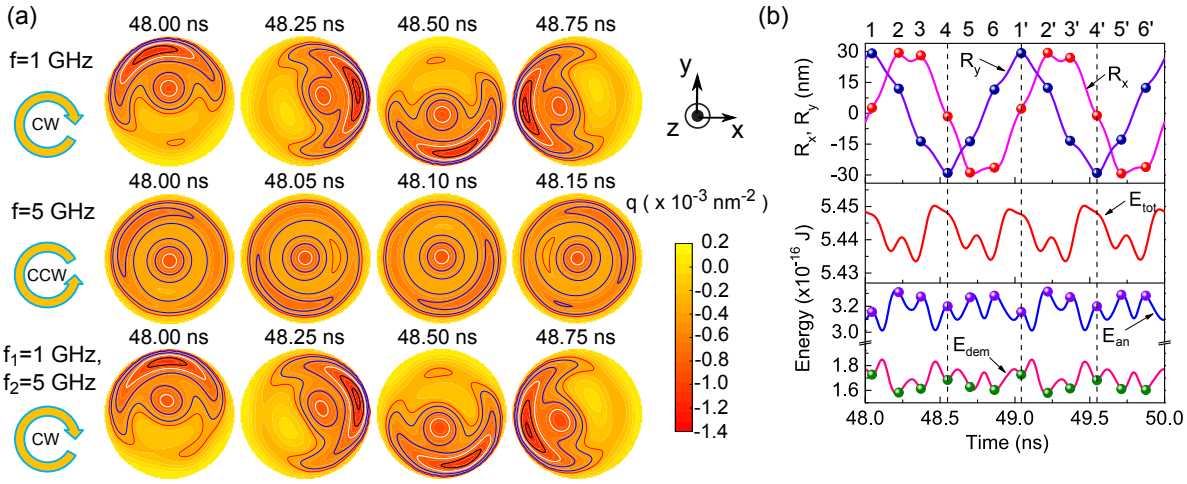

Fig. 2 (Color online) (a) The variation of topological density for the top nanolayer in one period under the different in-plane microwave magnetic fields. (b) The time dependence of R_x, R_y, the total (E_{tot}), uniaxial anisotropy (E_{an}) and demagnetization (E_{dem}) energies in two periods for the hexagonal steady orbit in Fig. 1d. Dots correspond to the cusps of the hexagon.

and 1c, respectively. The frequencies of the external field are chosen to be the eigenfrequencies of a hexagonal trajectory for gyrotropic motion of coupled skyrmions.[18] Both resonant orbits are approximately circular, and radius of 30.5 nm in Fig. 1b is much larger than that of 3.3 nm in Fig. 1c. We find that directions of their circulation are opposite, clockwise (CW) for the lower frequency mode while counterclockwise (CCW) for higher frequency mode. Compared with the resonant excitation of vortices,[30,38] the rotation of skyrmion depends not only on their polarities, but also strongly on the frequency of the microwave field due to their global spin textures. Mochizuki[39] has studied the microwave-absorption spectra of a two-dimensional model, where a skyrmion crystal is stabilized by the Dzyaloshinsky-Moriya interaction (DMI). It turned out that for twofold spin-wave modes, with a small microwave magnetic field, the frequency difference of the two modes is small. However, we find that with the effective mass, eqn (3), the two resonant excitation modes, far from being degenerate, exhibit a large frequency difference. When a dual-frequency microwave field $H_1 sin(2\pi f_1 t) + H_2 sin(2\pi f_2 t)$ with f_1 = 1 GHz and f_2 = 5 GHz is applied, the resonant trajectory of excitation is a hypocycloid, reminiscent of a hexagon instead of a circle as shown in Fig. 1d. Circular or elliptical, or even stadium-like orbits are common, while a hexagon is unusual in resonant excitation of vortices.[37,38] Interestingly, comparing the trajectory of guiding center in the dual-frequency field with the sum trajectory of that in the two single-frequency field, one can observe differences of amplitude and phase (about 12 degree), which indicates that two excitation modes are coupled with each other. The inset of Fig. 1d shows that the dynamical phase difference keeps unchanged when the contribution of higher-frequency mode was increased.

To comprehend the striking features of hexagonal resonant excitation, Fig. 2a shows time evolution of the topological density in one period for the steady orbits in Figs. 1b-1d. All the topological density distributions display a large nonlocal deformation, unlike very small and local deformations in vortex cores or in the narrow walls of bubbles.[35,40] Clearly, this global deformation rotates like a rigid body, suggesting that the effective mass associated with deformation of topological density shall be included to describe dynamics of coupled skyrmions. The direction of rotation for the lower-frequency mode is CW, while that for the higher-frequency one is CCW, which consists with the results in Figs. 1b-1d. When the dual-frequency microwave magnetic field is applied, the rotation direction is CW and the distribution of topological density is similar to that of the lower-frequency mode with a slight difference, indicating that the hexagon is a superposition of CW and CCW modes with the CW mode dominating.

In order to elucidate the contribution of competition between different energies to stabilize the hexagonal trajectory, Fig. 2b shows the energies of skyrmions as a function of time. Dots correspond to the six cusps of the hexagon labeled in Fig. 1d. Obviously, R_x, R_y and energies vary periodically with time and the periods are about 1 ns. Uniaxial anisotropy (E_{an}) and demagnetization (E_{dem}) energies take the most part of total energy. Interestingly, variation of E_{tot} is almost one order smaller than that of both E_{an} and E_{dem}, suggesting competition between E_{an} and E_{dem} plays a substantial role in determining the stable hexagonal trajectory. At each cusp, E_{dem} locates valley and E_{an} locates peak, whereas E_{dem}

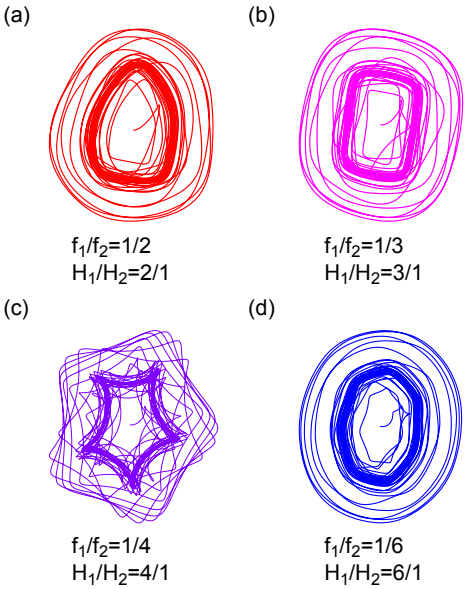

Fig. 3 (Color online) Transformation of topological resonant trajectory of the guiding center in different microwave magnetic fields with the waveform $H_1 sin(2\pi f_1 t) + H_2 sin(2\pi f_2 t)$. (a), (b), (c), (d) f_1 is chosen to be 1.15 GHz and the ratio of f_1/f_2 is 1/2, 1/3 1/4 and 1/6, respectively. The corresponding ratio of H_1/H_2 is 2/1, 3/1, 4/1, and 6/1, respectively. Amplitude H_1 is 50 Oe.

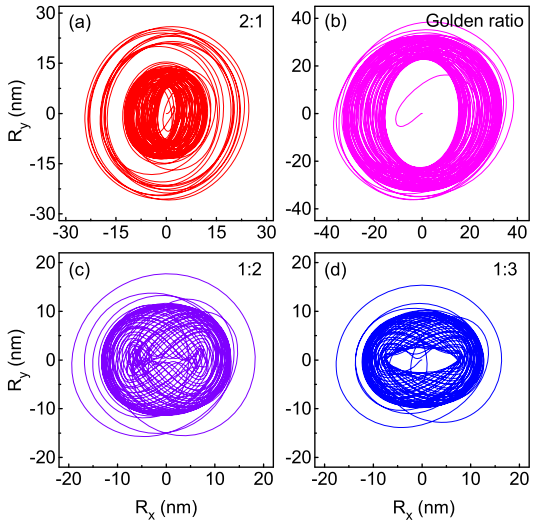

Fig. 4 (Color online) The quasiperiodic behavior of resonant excitation of skyrmion in a microwave magnetic field with frequency f_1 = 1.15 GHz and f_1/f_2 = 1/golden ratio. (a), (b), (c), (d) The corresponding amplitude ratio H_1/H_2 is 2/1, golden ratio, 1/2, and 1/3, respectively. Amplitude H_1 is 50 Oe.

reaches maximum and E_{an} reaches minimum between two cusps. The above analysis is also applicable to other types of polygonal trajectories.

We have demonstrated that resonant excitation can be used to transform the rotational trajectory of skyrmion from an approximately circle to a hexagon by switching a single-frequency microwave field to a dual-frequency one. Here we further show in Fig. 3 that tuning frequency ratio of the dual-frequency microwave field is also beneficial for the controllability of skyrmion dynamics. The frequency f_1 is chosen to be 1.15 GHz, which is the eigenfrequency of a circular trajectory for gyrotropic motion of coupled skyrmions. In the microwave field with the eigenfrequency, dynamics of skyrmion will exhibit a strong resonant excitation. Based on the strong resonant excitation, polygon-like trajectories can be obtained by tuning the frequency ratio of the dual-frequency field. The frequency ratio f_1/f_2 is 1/2, 1/3, 1/4 and 1/6, whereas the amplitude ratio is 2/1, 3/1, 4/1, and 6/1 in Figs. 3a-3d, respectively. The figures show the steady orbit of the topological resonant excitation is indeed able to be transformed from hexagon to other polygons such as triangle, quadrangle, pentagon, and heptagon. Such controllability of resonant excitation in nanoscale by means of a dual-frequency microwave field would be useful to manipulation of skyrmions and design of microwave devices.

In Fig. 4, the resonant excitation of skyrmion shows quasiperiodic behavior when an incommensurate frequency ratio (i.e. the golden ratio ($\sqrt{5}$-1)/2) of the microwave magnetic field is chosen. To note that it is not possible to use a true irrational number in simulations, here we used a rational number with precision up to 16 significant decimal digits for the golden ratio ($\sqrt{5}$-1)/2 and checked the result is insensitive to the number of digits if the decimal digits goes higher than 10. The trajectories of resonant excitations in a single-frequency (rational number) microwave field are periodic circles. After introduced microwave field with an irrational-number frequency, the system began to display quasiperiodicity. With the increase of amplitude ratio H_1/H_2, the trajectories become more uncertain due to increasing effect of irrational-number frequency. The nonlinear dynamical behavior was also found in a josephson-junction system under two ac sources, when the frequency ratio is a golden section.[41]

We have to point out that coupling between two skyrmions also plays a crucial role in the stability and controllability of coupled skyrmion dynamics, as illustrated in eqn (2) and eqn (4). Fig. 5 shows the influence of coupling on the trajectories and on the topological density distributions of skyrmions. Firstly, two guiding centers are driven away by an external constant magnetic field along the +x direction to $\pm$ 30 nm for top and bottom skyrmions, respectively, as labeled by dark diamonds in Fig. 5a. The guiding centers of two skyrmions move in opposite directions due to different chiralities and are finally decoupled. Then a dual-frequency microwave magnetic field (f_1/f_2=1/5 and H_1/H_2=5/1) replacing the constant

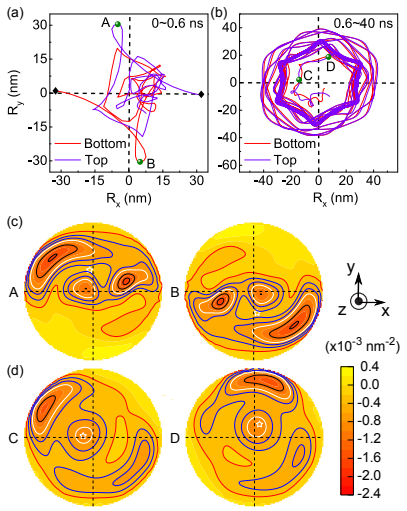

Fig. 5 (Color online) (a) and (b) Trajectories of the guiding centers of two skyrmions in 0∼0.6 ns and 0.6∼40 ns, respectively, after replacing an applied constant magnetic field with the dual-frequency microwave field. Dark diamonds in (a) show the positions of two guiding centers at 0 ns. (c) and (d) The topological density distributions of points A (0.035 ns on top nanolayer), B (0.035 ns on bottom nanolayer), C (1.008 ns on top nanolayer) and D (1.216 ns on top nanolayer) labeled in (a) and (b), respectively. The white stars in (c) and (d) represent positions of the guiding center.

field drives the two skyrmions to rotate. During 0∼0.6 ns, the two guiding centers of skrymions keep at diagonal position from each other but with the same rotation direction of CCW. The trajectories are quadrangles other than hexagon, quite complex and unstable as shown in Fig. 5a. The topological density distributions of points A and B labeled in Fig. 5a also show complicated patterns and large deformations in Fig. 5c. When getting close to each other at 0.6 ns due to a damping effect, the guiding centers of skyrmions are coupled. Consequently, their rotation senses change from CCW to CW, and hexagonal trajectories revive, as shown in Fig. 5b. Compared with the topological density distributions at initial time, those of the coupled skyrmions shown in Fig. 5d start to take a shape similar to the stable ones previously shown in Fig. 2a, and rotate as a relative rigid body from point C to D (labeled in Fig. 5b). Changing of the rotation direction indicates that skyrmion dynamics depends not only on their polarities, but also on the eigenfrequencies of circulation, which is distinguished from vortex. The results also indicate that the coupling between skyrmions can be used to manipulate topological density distribution, thus having influence on effective mass and on dynamics of the system.

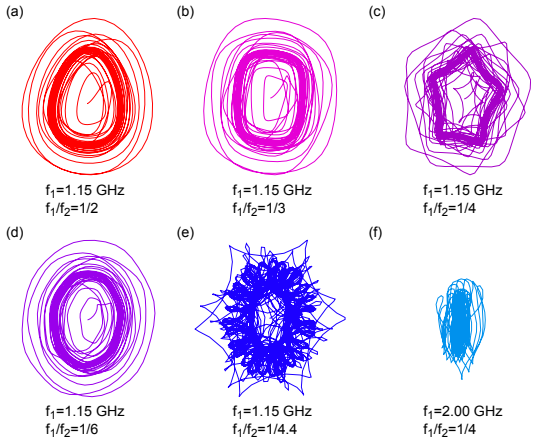

Fig. 6 (Color online) Numerical solutions to eqn (5) and eqn (6) for skyrmion driven by a dual-frequency field $H_x = H_1 sin(2\pi f_1 t) + H_2 sin(2\pi f_2 t)$. The values of f_1, frequency ratio f_1/f_2 and the corresponding H_1/H_2 are (a) 1.15 GHz, 1/2 and 2/1, (b) 1.15 GHz, 1/3 and 3/1, (c) 1.15 GHz, 1/4 and 4/1, (d) 1.15 GHz, 1/6 and 6/1, (e) 1.15 GHz, 1/4.4 and 4.4/1, (f) 2.00 GHz, 1/4 and 4/1, respectively.

3.3 Numerical Solutions to the Extended Thiele's Equation

To understand the polygon-like resonant excitations of coupled skyrmions under a dual-frequency microwave field, numerical solutions to eqn (2) were obtained by the Runge-Kutta method for different frequency ratios, as shown in Fig. 6. Because of the two skyrmions moving almost synchronously, we can use an effective potential energy to replace the total potential energy of one skyrmion. Eqn (2) with dissipation term considered for dynamics of skyrmion in the top nanodisk can be rewritten as follows:

$$\mu H_x - KR_x - G\dot{R}_y - D\dot{R}_x = M\ddot{R}_x, \quad (5)$$

$$-KR_y + G\dot{R}_x - D\dot{R}_y = M\ddot{R}_y, \quad (6)$$

where K is the effective stiffness coefficient and D the damping parameter.[36] Here, for numerical solutions to eqn (5) and eqn (6), $D = 5.59 \times 10^{-14}$ J s/m^2, $G = 4\pi M_s L/\gamma = 1.8 \times 10^{-12}$ J s/m^2 and $\mu = \pi\mu_0 RLM_s\xi = 1.0 \times 10^{-14}$ kg m^2/(As^2) with $\xi \approx 0.93$ for skyrmion in this work.[36] Values of K (0.013 J/m^2) and M (7.08×10^{-23} kg) are calculated under zero field according to the eigenfrequencies of near 0.96 and 4.98 GHz for hexagonal trajectory of gyrotropic motion and 1.15 GHz for circular one.[18,40]

Polygon-like resonant excitations can be driven by a dual-frequency field $H_x = H_1 sin(2\pi f_1 t) + H_2 sin(2\pi f_2 t)$ with f_1 of 1.15 GHz (one of the eigenfrequency of skyrmion) and f_2 as an integral multiple of f_1, as shown in Figs. 6a-6d. The polygonal trajectories from numerical solution are in best agreement with those from micromagnetic simulations (Fig. 3).

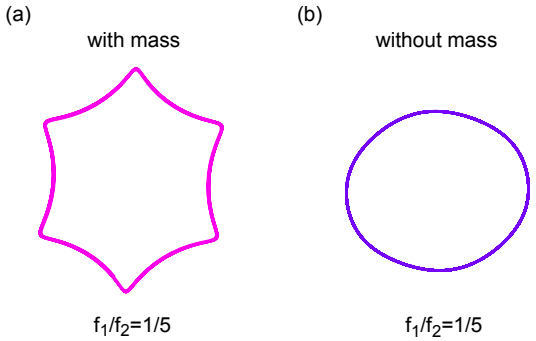

Fig. 7 (Color online) Numerical solutions to eqn (5) and eqn (6) for skyrmion driven by a dual-frequency field $H_x = H_1 sin(2\pi f_1 t) + H_2 sin(2\pi f_2 t)$ with f_1 of 1.00 GHz (a) with and (b) without the effective mass term considered. The frequency ratio f_1/f_2 is 1/5, and the amplitude ratio H_1/H_2 is 5/1. Only steady trajectories are shown here.

When f_2 is a non-integral multiple of f_1, a polygon-like orbit cannot be obtained. As an example, Fig. 6e illustrates resonant excitation of skyrmion in a field with f_1/f_2 of 1/4.4, which gives a different result from polygon-like resonance, indicating that the resonant dynamics of skyrmion is sensitive to the frequency ratio of the dual-frequency field.

Actually, not only the frequency ratio, but also the value of frequency are of great importance to the dynamics of skyrmion. Dynamics of skyrmions will show neither a strong resonance, nor polygon-like trajectory, if the frequency of the external field is not equal nor close to the eigenfrequency of skyrmion. To confirm it, Fig. 6f demonstrates the trajectory of skyrmion in a field with frequency f_1 of 2.00 GHz, which is far away from the eigenfrequency of skyrmion. In this case, though a dual-frequency field is applied, dynamics of skyrmion does not show a polygon-like behavior.

To clarify the importance of the effective mass to the polygon-like dynamics of skyrmion, Fig. 7 shows the numerical solutions to eqn (5) and eqn (6) with and without the effective mass term. Parameters of eqn (5) and eqn (6) in Fig. 7 are the same as used in Fig. 6. An external field with f_1 of 1.00 GHz (one of the eigenfrequencies of coupled skyrmions), f_1/f_2 of 1/5 and H_1/H_2 of 5/1 is applied on the system. Fig. 7a demonstrates the steady orbit of the numerical solution as the effective mass is considered. A hexagonal trajectory is obtained, which agrees well with the result of Fig. 1d from the micromagnetic simulation. However, when the effective mass term is not considered, the result is totally different and an approximately circular trajectory obtained as shown in Fig. 7b. The results indicate that the effective mass is vital to the polygon-like trajectory.

From Figs. 6 and 7, the factors governing the polygon-like excitations of skyrmion can be listed as follows: (1) The frequency f_1 of the external field has to be equal or close to the eigenfrequency of skyrmion. (2) A dual-frequency field with an integer frequency ratio f_2/f_1 is necessary. (3) The effective mass of skyrmion associated with time derivative of topological density is important to the polygon-like resonant excitations.

Note that twofold spin-wave modes excitation under a small microwave field are theoretically anticipated while only low-frequency mode has been experimentally observed. High-frequency mode may be mixed with helical mode or indistinguishable from breathing mode due to their similar resonance frequencies.[22,39,42] Compared with the spin-wave modes, two modes of topological resonant excitations in present work have higher frequencies and larger frequency difference. Moreover, there is no existence of conical mode for Co/Ru/Co nanodisks. Therefore, we expect that the topological resonant modes are to be found in experiment and may contribute to the understanding of the collective excitation in skyrmions.

4 Conclusions

In conclusion, we have numerically studied the resonant excitation of two coupled skyrmions in Co/Ru/Co nanodisks by micromagnetic simulations. Thiele's equation of guiding center incorporating an effective mass term is used to comprehend two coupled resonant modes of skyrmions with nonlocal deformation. Rotational trajectories have been controllably transformed from circular to different polygonal shapes by tuning commensurate frequency ratio of a dual-frequency microwave field with f_1 chosen to be the eigenfrequency of skyrmion. Quasiperiodic behavior of skyrmion dynamics is observed when the frequency ratio is incommensurate. Numerical solution to the extended Thiele's equation clarifies the importance of the value of f_1, the frequency ratio f_1/f_2 of a dual-frequency field and the effective mass to the polygon-like resonant excitations of skyrmion. We have also shown the coupling between two skyrmions has an obvious effect on their dynamics. These findings contribute to a better understanding of skyrmion dynamics and may open a new avenue to the manipulation of spin textures in nanoscale by a dual-frequency microwave field.

Acknowledgements

We appreciate helpful discussions with Prof. Peter F. de Chatel. The work is supported by the National Basic Research Program (No. 2010CB934603) of China, Ministry of Science and Technology China and the National Natural Science Foundation of China under Grant No. 51331006.

References

1 I. K. Schuller, S. Kim and C. Leighton, *J. Magn. Magn. Mater.*, 1999, **200**, 571 – 582.

2 M. R. Fitzsimmons, S. D. Bader, J. A. Borchers, G. P. Felcher, J. K. Furdyna, A. Hoffmann, J. B. Kortright, I. K. Schuller, T. C. Schulthess, S. K. Sinha, M. F. Toney, D. Weller and S. Wolf, *J. Magn. Magn. Mater.*, 2004, **271**, 103 – 146.

3 J. Fu, J. Zhang, Y. Peng, J. Zhao, G. Tan, N. J. Mellors, E. Xie and W. Han, *Nanoscale*, 2012, **4**, 3932–3936.

4 M. S. Salem, P. Sergelius, R. M. Corona, J. Escrig, D. Görlitz and K. Nielsch, *Nanoscale*, 2013, **5**, 3941–3947.

5 S.-B. Choe, Y. Acremann, A. Scholl, A. Bauer, A. Doran, J. Stöhr and H. A. Padmore, *Science*, 2004, **304**, 420–422.

6 J. P. Park, P. Eames, D. M. Engebretson, J. Berezovsky and P. A. Crowell, *Phys. Rev. B*, 2003, **67**, 020403.

7 C. Phatak, A. K. Petford-Long and O. Heinonen, *Phys. Rev. Lett.*, 2012, **108**, 067205.

8 H. Jung, K.-S. Lee, D.-E. Jeong, Y.-S. Choi, Y.-S. Yu, D.-S. Han, A. Vogel, L. Bocklage, G. Meier, M.-Y. Im, P. Fischer and S.-K. Kim, *Sci. Rep.*, 2011, **1**, 59.

9 A. Dussaux, B. Georges, J. Grollier, V. Cros, A. V. Khvalkovskiy, A. Fukushima, M. Konoto, H. Kubota, K. Yakushiji, S. Yuasa, K. A. Zvezdin, K. Ando and A. Fert, *Nat. Commun.*, 2010, **1**, 8.

10 V. S. Pribiag, I. N. Krivorotov, G. D. Fuchs, P. M. Braganca, O. Ozatay, J. C. Sankey, D. C. Ralph and R. A. Buhrman, *Nat. Phys.*, 2007, **3**, 498–503.

11 S. Mühlbauer, B. Binz, F. Jonietz, C. Pfleiderer, A. Rosch, A. Neubauer, R. Georgii and P. Böni, *Science*, 2009, **323**, 915–919.

12 X. Z. Yu, Y. Onose, N. Kanazawa, J. H. Park, J. H. Han, Y. Matsui, N. Nagaosa and Y. Tokura, *Nature*, 2010, **465**, 901–904.

13 X. Z. Yu, N. Kanazawa, Y. Onose, K. Kimoto, W. Z. Zhang, S. Ishiwata, Y. Matsui and Y. Tokura, *Nat. Mater.*, 2011, **10**, 106 – 109.

14 T. Adams, S. Mühlbauer, C. Pfleiderer, F. Jonietz, A. Bauer, A. Neubauer, R. Georgii, P. Böni, U. Keiderling, K. Everschor, M. Garst and A. Rosch, *Phys. Rev. Lett.*, 2011, **107**, 217206.

15 S. Heinze, K. von Bergmann, M. Menzel, J. Brede, A. Kubetzka, R. Wiesendanger, G. Bihlmayer and S. Blügel, *Nat. Phys.*, 2011, **7**, 713 – 718.

16 I. Raičević, D. Popović, C. Panagopoulos, L. Benfatto, M. B. Silva Neto, E. S. Choi and T. Sasagawa, *Phys. Rev. Lett.*, 2011, **106**, 227206.

17 S. Seki, X. Z. Yu, S. Ishiwata and Y. Tokura, *Science*, 2012, **336**, 198–201.

18 Y. Y. Dai, H. Wang, P. Tao, T. Yang, W. J. Ren and Z. D. Zhang, *Phys. Rev. B*, 2013, **88**, 054403.

19 L. Sun, R. X. Cao, B. F. Miao, Z. Feng, B. You, D. Wu, W. Zhang, A. Hu and H. F. Ding, *Phys. Rev. Lett.*, 2013, **110**, 167201.

20 J. Li, A. Tan, K. W. Moon, A. Doran, M. A. Marcus, A. T. Young, E. Arenholz, S. Ma, R. F. Yang, C. Hwang and Z. Q. Qiu, *Nat. Commun.*, 2014, **5**, 4704.

21 C. Pfleiderer and A. Rosch, *Nature*, 2010, **465**, 880 – 881.

22 Y. Okamura, F. Kagawa, M. Mochizuki, M. Kubota, S. Seki, S. Ishiwata, M. Kawasaki, Y. Onose and Y. Tokura, *Nat. Commun.*, 2013, **4**, 2391.

23 F. Jonietz, S. Mühlbauer, C. Pfleiderer, A. Neubauer, W. Münzer, A. Bauer, T. Adams, R. Georgii, P. Böni, R. A. Duine, K. Everschor, M. Garst and A. Rosch, *Science*, 2010, **330**, 1648–1651.

24 X. Z. Yu, N. Kanazawa, W. Z. Zhang, T. Nagai, T. Hara, K. Kimoto, Y. Matsui, Y. Onose and Y. Tokura, *Nat. Commun.*, 2012, **3**, 988.

25 J. Iwasaki, M. Mochizuki and N. Nagaosa, *Nat. Commun.*, 2013, **4**, 1463.

26 J. Iwasaki, M. Mochizuki and N. Nagaosa, *Nat. Nanotechnol.*, 2013, **8**, 742–747.

27 Y. Zhou and M. Ezawa, *Nat. Commun.*, 2014, **5**, 4652.

28 B. Van Waeyenberge, A. Puzic, H. Stoll, K. W. Chou, T. Tyliszczak, R. Hertel, M. Fähnle, H. Brückl, K. Rott, G. Reiss, I. Neudecker, D. Weiss, C. H. Back and G. Schütz, *Nature*, 2006, **444**, 461–464.

29 K. Yamada, S. Kasai, Y. Nakatani, K. Kobayashi, H. Kohno, A. Thiaville and T. Ono, *Nat. Mater.*, 2007, **6**, 269–273.

30 S.-K. Kim, K.-S. Lee, Y.-S. Yu and Y.-S. Choi, *Appl. Phys. Lett.*, 2008, **92**, 022509.

31 Y. Dai, H. Wang, T. Yang, W. Ren and Z. Zhang, *Sci. Rep.*, 2014, **4**, 6135.

32 M. J. Donahue and D. G. Porter, *OOMMF User's Guide, Version 1.2a5*, 2012.

33 P. J. H. Bloemen, H. W. van Kesteren, H. J. M. Swagten and W. J. M. de Jonge, *Phys. Rev. B*, 1994, **50**, 13505–13514.

34 N. Papanicolaou and T. N. Tomaras, *Nucl. Phys. B*, 1991, **360**, 425 – 462.

35 G. M. Wysin, F. G. Mertens, A. R. Völkel and A. R. Bishop, in *Nonlinear Coherent Structures in Physics and Biology,* ed. K. H. Spatschek and F. G. Mertens, Plenum Press, New York, 1993.

36 K. Yu. Guslienko, *Appl. Phys. Lett.*, 2006, **89**, 022510.

37 K.-S. Lee and S.-K. Kim, *Appl. Phys. Lett.*, 2007, **91**, 132511.

38 S. Kasai, Y. Nakatani, K. Kobayashi, H. Kohno and T. Ono, *Phys. Rev. Lett.*, 2006, **97**, 107204.

39 M. Mochizuki, *Phys. Rev. Lett.*, 2012, **108**, 017601.

40 I. Makhfudz, B. Krüger and O. Tchernyshyov, *Phys. Rev. Lett.*, 2012, **109**, 217201.

41 D.-R. He, W. J. Yeh and Y. H. Kao, *Phys. Rev. B*, 1984, **30**, 172–178.

42 Y. Onose, Y. Okamura, S. Seki, S. Ishiwata and Y. Tokura, *Phys. Rev. Lett.*, 2012, **109**, 037603.

Dual-frequency Microwave-driven Resonant Excitations of Skyrmions in Nanoscale magnet

HanWang, Yingying Dai, Teng Yang,Weijun Ren and Zhidong Zhang

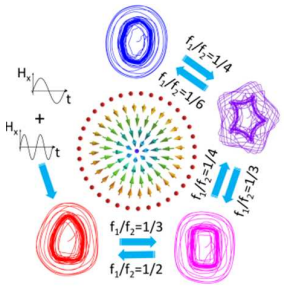

Polygon-like resonant excitations of coupled skyrmions can be controlled in nanoscale by a dual-frequency microwave field.